

## QUANTITATIVE GENETICS OF GEOMETRIC SHAPE IN THE MOUSE MANDIBLE

CHRISTIAN PETER KLINGENBERG<sup>1,2</sup> AND LARRY J. LEAMY<sup>3,4</sup>

<sup>1</sup>Laboratory for Development and Evolution, University Museum of Zoology, Department of Zoology, Downing Street, Cambridge CB2 3EJ, United Kingdom

<sup>3</sup>Department of Biology, University of North Carolina at Charlotte, Charlotte, North Carolina 28223

<sup>4</sup>E-mail: ljleamy@email.uncc.edu

**Abstract.**—We combine the methods of geometric morphometrics and multivariate quantitative genetics to study the patterns of phenotypic and genetic variation of mandible shape in random-bred mice. The data are the positions of 11 landmarks on the mandibles of 1241 mice from a parent-offspring breeding design. We use Procrustes superimposition to extract shape variation and restricted maximum likelihood to estimate the additive genetic and environmental components of variance and covariance. Matrix permutation tests showed that the genetic and phenotypic as well as the genetic and environmental covariance matrices were similar, but not identical. Likewise, principal component analyses revealed correspondence in the patterns of phenotypic and genetic variation. Patterns revealed in these analyses also showed similarities to features previously found in the effects of quantitative trait loci and in the phenotypes generated in gene knockout experiments. We used the multivariate version of the breeders' equation to explore the potential for short-term response to selection on shape. In general, the correlated response is substantial and regularly exceeds the direct response: Selection applied locally to one landmark usually produces a response in other parts of the mandible as well. Moreover, even selection for shifts of the same landmark in different directions can yield dramatically different responses. These results demonstrate the role of the geometry and anatomical structure of the mandible, which are key determinants of the patterns of the genetic and phenotypic covariance matrices, in molding the potential for adaptive evolution.

**Key words.**—Additive genetic covariance matrix, constraint, correlated response, geometric morphometrics, heritability, restricted maximum likelihood, shape analysis.

Received February 9, 2001. Accepted July 15, 2001.

The evolution of morphological structures by natural selection depends on the availability of genetic variation for the traits in question. Particularly for multidimensional features such as shape, the response to selection depends critically on the patterns of genetic and phenotypic variation, as they are represented by the additive genetic and phenotypic covariance matrices (Lande 1979; Cheverud 1984). Therefore, estimation of those covariance matrices has long been a central part of evolutionary quantitative genetics (e.g., Roff 1997; Lynch and Walsh 1998).

Just as important as estimating the components of variance and covariance, however, is the choice of a method for characterizing morphological form. Conventionally, this has been done by analyzing sets of linear distances measured on each specimen. In the past two decades, however, several new methods have been developed that emphasize the geometry of a morphological structure and are based either on outline contours or the arrangement of landmark points (e.g., Bookstein 1991, 1996; Dryden and Mardia 1998). Here, we demonstrate the use of landmark-based morphometrics in the context of a quantitative genetic study of mouse mandible shape.

The rodent mandible is composed of several parts that are morphologically recognizable and have distinct developmental origins (Fig. 1), and it has long been used as a model for genetics, development, and evolution of complex morphological structures (Atchley and Hall 1991; Hall 1999, p. 323 ff.). Studies of the mandible in mice and other rodents have focused on a variety of specific contexts, and together provide a multifaceted picture of its development and evolutionary

potential. Morphometric analyses comparing different laboratory strains, natural populations, or species have shown that evolutionary change differentially affects the various parts of the mandible (Cheverud et al. 1991; Atchley et al. 1992; Duarte et al. 2000). Likewise, analyses of congenic and recombinant-inbred strains (Bailey 1985, 1986) and studies of quantitative trait loci (QTLs; e.g., Cheverud et al. 1997; Mezey et al. 2000; Cheverud 2001; Klingenberg et al. 2001b) suggest that the effect of each locus is usually localized in specific regions of the mandible. The classical methods of quantitative genetics, which consider the aggregate effect of all segregating loci that affect mandible shape simultaneously, also reveal similarly regionalized variation (Atchley et al. 1985). Finally, the correlated response of mandibular traits to artificial selection on body composition provides further evidence for this spatially patterned nature of genetic variation in the mandible (Atchley et al. 1990).

To investigate the spatial organization of genetic variation in more detail, we combine the methods of geometric morphometrics with those of evolutionary quantitative genetics. This combination of approaches allows us to depict the patterns of variation in the phenotypic and genetic covariance matrices. By using the algebra of the multivariate generalization of the breeders' equation (Lande 1979; Cheverud 1984; Cowley and Atchley 1990), we can make predictions about the short-term response to selection on various features of shape. These analyses highlight the dependence of selection response on the geometry of the mandible. We relate the results of the present analyses to patterns of gene effects identified in a QTL study using the same geometric approach (Klingenberg et al. 2001b), and we discuss them in the light of previous work on morphological integration among the parts of the mandible (e.g., Atchley and Hall 1991; Cheverud 1996; Cheverud et al. 1997; Mezey et al. 2000).

<sup>2</sup> Present address: Department of Biology, University of Konstanz, 78457 Konstanz, Germany; E-mail: Christian.Klingenberg@uni-konstanz.de.

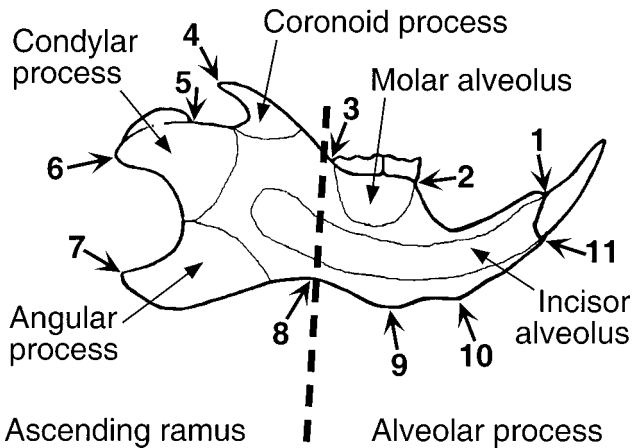


FIG. 1. Diagram of a mouse mandible indicating the major anatomical parts and the locations of the 11 landmarks included in this study.

## MATERIALS AND METHODS

### Breeding Design and Data Collection

The mice (*Mus musculus*) used in this study are from the random-bred laboratory mouse strain CV1 (for details on the origin of this strain, see Leamy 1974), and this set of mice has been the subject of several previous studies (e.g., Leamy 1974, 1977, 1993, 1999; Leamy and Bradley 1982). The study was set up as a parent-offspring design with 200 breeding pairs (for further details, see Leamy 1974). All mice were maintained in an animal room at room temperature and with food (Purina mouse chow) and water available ad libitum. Offspring are first litters of the parental animals, and larger litters were reduced to six individuals within two days of birth. Two offspring of each litter were killed at 35 days, 3 months, and 5 months after birth, and all parents were killed at 5 months of age. Skeletons of all individuals were prepared by exposure to dermestid beetles.

The left and right hemimandibles were separated at the mandibular symphysis. Each was placed separately on a glass slide in a photographic enlarger and projected onto a digitizing tablet to record the  $x$  and  $y$  coordinates of a set of morphological landmarks. In this study, we included 11 landmarks located around the outline of the mandible (Fig. 1). After eliminating all animals with incomplete data and removing the outliers revealed by preliminary shape analyses based on the criterion of standard distance (Flury 1997, pp. 188 f.), this study used information from 197 families. These families contained a total of 1309 individuals, of which the complete morphometric data were available from 1241 individuals. There was substantial imbalance in the design, however, as the complete information on both parents and six offspring was available for only 45 families, whereas the remaining ones had fewer offspring or missed one or both parental animals.

### Analysis of Size and Shape

Geometric morphometrics separates morphological variation into components of size and shape (Bookstein 1991, 1996; Dryden and Mardia 1998). Size is a scalar (one-di-

mensional) feature of a configuration of landmarks, and is measured in units of distance (millimeters). It therefore can be treated like any length measurement used as a trait in conventional studies of quantitative genetics. We used centroid size as the measure of size, which was computed as the square root of the sum of squared distances of each landmark from the centroid (center of gravity) of all the landmarks of a specimen (e.g., Dryden and Mardia 1998, p. 24).

Shape encompasses all those features of a configuration of landmarks that are invariant to scaling (variation in size), translation (variation in the position of the specimen on the digitizing tablet), and rotation (variation in the orientation of the specimen). Shape is therefore inherently multidimensional in nature. To characterize shape variation we used Procrustes superimposition. This method extracts the shape information from the original landmark configurations by scaling to unit centroid size, superimposing the centroids of all configurations, and rotating the configurations to a position of optimal fit according to a least-squares criterion (e.g., Bookstein 1996; Dryden and Mardia 1998). Because the dataset included both left and right hemimandibles, which are mirror images of one another, our analyses also removed the differences due to reflection (for a more detailed explanation, see Klingenberg and McIntyre 1998). The reflection, scaling, and superimposition steps are performed for all specimens simultaneously (we used a full Procrustes fit and projection onto a tangent space; Dryden and Mardia 1998, pp. 44, 74).

Even though left and right sides were measured separately, we did not analyze asymmetry in this study (for studies of asymmetry in these mice, see Leamy 1993, 1999). Instead, we focused entirely on interindividual variation by averaging the coordinates of the left and right hemimandibles of each mouse after Procrustes superimposition (thereby minimizing the effect of measurement error; Klingenberg and McIntyre 1998). The resulting average landmark coordinates for each individual were then entered into standard multivariate procedures for the genetic analysis. Because the Procrustes superimposition eliminates variation in scale, position, and orientation, the dimensionality of the data is reduced from  $2k$  to  $2k - 4$ , where  $k$  is the number of landmarks included (i.e., for the present study of 11 landmarks, with 22 coordinates, the shape dimension is 18). Therefore, special care should be taken whenever the analyses involve matrix inversion (e.g., by using generalized inverses; Dryden and Mardia 1998, p. 152).

It is important to keep in mind that shape is a multivariate feature and cannot be easily divided into scalar traits without imposing arbitrary constraints on the results of the analyses. In particular, such constraints are inherent in the practice of choosing shape variables a priori and then estimating quantitative genetic parameters for these. Throughout this study, we therefore used multivariate analyses of shape and only present the final results, such as principal components (PCs), as single features of shape (for further explanations, see Klingenberg and McIntyre 1998; Klingenberg and Zaklan 2000; Klingenberg et al. 2001b). To maintain the scale inherent in the geometry for all coordinates, regardless of the amount of variation of landmarks in each direction, we consistently use covariance and not correlation matrices (e.g., Klingenberg

and Zaklan 2000); moreover, covariance matrices are required for the multivariate breeders' equation (Lande 1979).

#### *Variance Component Estimation and Analysis*

In recent years, restricted maximum likelihood (REML) has emerged as the preferred method for estimating variance components from the mixed models used in quantitative genetic studies (e.g., Shaw 1987; Lynch and Walsh 1998). Because this approach uses all the available information about relationships among individuals included, for example parent-offspring and full-sibling relations, it can easily accommodate unbalanced or nonstandard designs, or it can even be used in the wild (Milner et al. 2000). In this study, missing data for both the parental and offspring generations caused substantial imbalance in the design (see above). To find the REML solutions, we used the method of analytical gradients as implemented in the software package VCE4 (Neumaier and Groeneveld 1998), which is freely available at <http://www.tzv.fal.de/institut/genetik/vce4/vce4.html>.

Although our study primarily focused on shape, we conducted a separate analysis for centroid size as well, because both size and shape are required to characterize the mandible completely. We used the following animal model (Lynch and Walsh 1998, ch. 26):

$$\mathbf{y} = \mathbf{X}\boldsymbol{\beta} + \mathbf{Z}_1\mathbf{a} + \mathbf{Z}_2\mathbf{m} + \mathbf{e}, \quad (1)$$

where  $\mathbf{y}$  is the vector of observations for each individual,  $\mathbf{X}$  is a design matrix, and  $\boldsymbol{\beta}$  is the vector of fixed effects. We included fixed effects for sex and age (because the parents were assigned an age code different from that of 5-month old offspring, this automatically accounted for differences between generations too). The combined analysis of both sexes and all age groups was possible because preliminary analyses did not indicate significant heterogeneity in the variation of mandible size or shape among age groups or sexes.  $\mathbf{Z}_1$  and  $\mathbf{Z}_2$  are incidence matrices,  $\mathbf{a}$  is the vector of breeding values (for the additive genetic effects), and  $\mathbf{m}$  is a vector of maternal effects and of effects of the common environment within litters (because the design contained a single litter per dam, we were not able to separate these effects). Finally,  $\mathbf{e}$  is a vector of residual deviations. VCE4 provided estimates of these components of variation as scalar additive genetic, dam, and residual variances for centroid size, from which heritability was then computed.

The analysis for shape was an extension of the genetic model for centroid size, using the equation above for each of the shape variables. However, the fixed effects in the analyses of shape also included centroid size as a covariate to control for the allometric effects of size. VCE4 provided estimates of the additive genetic, maternal (or litter environmental), and residual covariance matrices for this model.

Our analyses have some limitations imposed by the available software and the inherent computational demands of the analyses. Whereas the VCE4 program has a substantial performance advantage due to its use of the method of analytical gradients (Neumaier and Groeneveld 1998), it also imposes some constraints. The current implementation of VCE4 (ver. 4.2.5, for OSF1 on a DEC Alpha system) is limited to a maximum of 15 dependent variables. To estimate the co-

variance components in a single analysis, which can account for all genetic or residual covariances simultaneously, we reduced the dimensionality of the shape data from 18 to 15 with principal component analysis (PCA). For presentation of the results, the same matrix of PC coefficients was used to convert the genetic, maternal, and residual covariance matrices returned by VCE4 back into the space of the original coordinates (in both coordinate systems, the phenotypic covariance matrix is the sum of the genetic and residual covariance matrices). The first 15 PCs accounted for 97.6% of the total shape variance in the data, indicating that the loss of variation due to the reduced dimensionality was negligible. Moreover, the results presented here are nearly identical to those from analyses of the complete 18-dimensional genetic and residual covariance matrices that we assembled from a series of VCE4 runs with different subsets of the landmark coordinates. However, analyses of datasets with more landmarks or three-dimensional data may be difficult.

Moreover, the program provides no measures of statistical uncertainty for the estimates of variance and covariance components, limiting the possibility for statistical tests of the shape features derived from them (VCE4 provides the standard errors for heritabilities and genetic or environmental correlations, but those cannot be used in this context). Furthermore, with the resources available to us, it was impossible to use the bootstrap or other resampling procedures to assess the statistical uncertainty of variance and covariance component estimates because the computational effort required was prohibitive (days or weeks of CPU time). These difficulties, although limiting for the present study, can be remedied in future releases of the software or circumvented as more powerful computing equipment becomes available. Of course, if it is possible to achieve a sufficiently large balanced design, least-squares methods can be used to estimate variance components, and these computational difficulties do not apply.

#### *Comparison of Covariance Matrices*

We used matrix correlations for overall comparison of the genetic and phenotypic covariance matrices, and we assessed their statistical significance with a matrix permutation test adapted to the specific situation in geometric morphometrics (Klingenberg and McIntyre 1998). We computed the matrix correlation, the correlation between corresponding elements of two matrices, including both the diagonal and off-diagonal elements of the matrices. For the matrix permutation procedure, the landmarks were randomly permuted, always keeping together the  $x$  and  $y$  coordinates of each landmark. For every matrix comparison, we ran 10,000 permutation iterations.

We used PCA to characterize the genetic and phenotypic covariance matrices and to display the dominant features of shape variation. The PCs are visualized as changes of the landmark configurations (scaled to an arbitrary magnitude of 0.1 units of Procrustes distance). To generate the corresponding deformation for an outline of the mandible, we used the thin-plate spline as an interpolation method (Bookstein 1991; Dryden and Mardia 1998, ch. 10). Comparisons of PCs between the genetic and phenotypic covariance matrices were

based on the vector correlations between the PCs, which are the inner products of corresponding PC vectors (each scaled to unit length, as usual for PCs), or equivalently, the angles between them (the angles are simply the arccosines of the respective vector correlations, but provide a more intuitive measure of similarity). A randomization test was used to test the observed statistics against the null hypothesis that the PCs were no more similar than pairs of random vectors. This test generated a null distribution by computing the absolute vector correlations for 10,000 pairs of random vectors in 15-dimensional space (e.g., Klingenberg 1996; Klingenberg and McIntyre 1998). Because we present comparisons for the first four PCs for each covariance matrix, we used a sequential Bonferroni adjustment to account for the 16 possible comparisons.

*Predicted Response to Selection*

The response to selection on shape can be predicted with the multivariate version of the breeders' equation:  $\Delta\mu = \mathbf{G}\mathbf{P}^{-1}\mathbf{s}$  (Lande 1979). In this equation,  $\Delta\mu$  is the response to selection, that is, the vector of differences in trait means between generations. The matrices  $\mathbf{G}$  and  $\mathbf{P}$  are the additive genetic and the phenotypic covariance matrix, respectively. Finally,  $\mathbf{s}$  is the vector of selection differentials, that is, the difference of the averages in the parental generation before and after selection, or, equivalently, the covariances between the shape variables and relative fitness (Lande and Arnold 1983). This equation can be applied with the estimates of the phenotypic and genetic covariance matrices from the present study (e.g., Cowley and Atchley 1990).

For shape data, it is important to use a generalized inverse of the phenotypic covariance matrix because it does not have full rank (i.e.,  $\Delta\mu = \mathbf{G}\mathbf{P}^{-}\mathbf{s}$ , where  $\mathbf{P}^{-}$  is the Moore-Penrose generalized inverse of  $\mathbf{P}$ ). Moreover, in this paper, presentation will focus on the selection differential  $\mathbf{s}$  rather than on the selection gradient  $\mathbf{P}^{-}\mathbf{s}$ , which has been emphasized in most regression analyses of selection (e.g., Lande and Arnold 1983; Mitchell-Olds and Shaw 1987), because  $\mathbf{s}$  (like  $\Delta\mu$ ) is a vector in shape space and therefore can be visualized and compared directly to the selection response. The transformation of  $\mathbf{s}$  to  $\mathbf{P}^{-}\mathbf{s}$  involves a rescaling of coordinate axes that corresponds to a distortion of the variation in the original configuration in different ratios and different directions at each landmark, it is impossible to display and interpret the selection gradient graphically in relation to the geometry of the mandible. Notice, however, that the selection differentials shown in this study therefore refer to the total selection and do not distinguish direct selection from selection that occurs via phenotypic correlation among shape variables (Lande and Arnold 1983).

First, we identify the aspect of mandible shape that most easily responds to selection, or, in other words, the selection differential  $\mathbf{s}$  (with a standard length  $\|\mathbf{s}\| = (\mathbf{s}'\mathbf{s})^{0.5}$ ) that yields the maximal response (measured in terms of length,  $\|\Delta\mu\|$ ). This selection differential can be computed as the dominant eigenvector of the matrix  $\mathbf{G}\mathbf{P}^{-}$ . The eigenvalue associated with this eigenvector is the ratio of the response to the selection differential, which is the realized heritability familiar from univariate studies (e.g., Falconer and Mackay 1996, p.

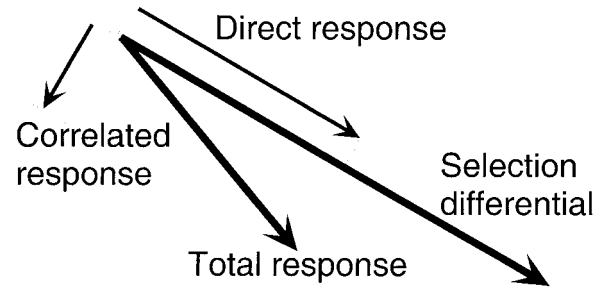


FIG. 2. Partition of the total response to selection into direct and correlated responses. The direct response is the component of the total response that is in the same direction in shape space as the vector of selection differentials, and the correlated response is the component perpendicular to it.

197 ff.). The univariate concept of heritability applies for this special case where the selection differential  $\mathbf{s}$  is an eigenvector of  $\mathbf{G}\mathbf{P}^{-}$ , because here  $\Delta\mu$  is a scalar multiple of  $\mathbf{s}$  (basically, this is a univariate problem in the direction of the vector  $\mathbf{s}$ ). The eigenvalues of  $\mathbf{G}\mathbf{P}^{-}$  can be used to assess the range of heritabilities for different shape variables and thus provide a link to studies that used one or more shape variables selected a priori (e.g., Arnqvist and Thornhill 1998). In principle, the same approach could also be used to identify the shape feature that shows the maximal genetic constraint, which would be the eigenvector of  $\mathbf{G}\mathbf{P}^{-}$  associated with the smallest eigenvalue. This is not possible here, however, because we eliminated the three shape dimensions with the smallest phenotypic eigenvalues. Moreover, eigenvectors associated with the smallest eigenvalues are expected to be worst affected by sampling error and numerical error in the estimation procedure.

We also examined the predicted responses to selection for six hypothetical selection differentials (see also Cowley and Atchley 1990). The selection differentials were designed to illustrate various aspects relevant to quantitative genetic studies of mandible shape (full descriptions are provided in the Results). Each of the selection differentials has an arbitrary length of 0.12 Procrustes units. This shape change would be unrealistically large for real selection experiments, but the resulting response shows the same spatial patterning and is visible without amplification. In each of the six examples, we partition the vector of the total response to selection into two components (Fig. 2): One component is in the same direction of shape space as the selection differential, reflecting the direct response, whereas the other component is perpendicular to it and constitutes the correlated response (shifts of different landmarks or shifts in different directions than in the selection differential). The two components can be quantified in terms of Procrustes distance: The magnitude of the direct response can be computed as  $\Delta\mu' \mathbf{s} / (\|\mathbf{s}\|)$ , and that of the correlated response can then be obtained from the total and direct response by the Pythagorean theorem.

For specifying the selection differentials used in these calculations, it was necessary to use some (arbitrary) convention to determine the anterior-posterior and dorsal-ventral directions. We established anterior-posterior direction to run from landmark 1 to the midpoint between landmarks 4 and 7 in the configuration of the Procrustes mean shape (drawn as the

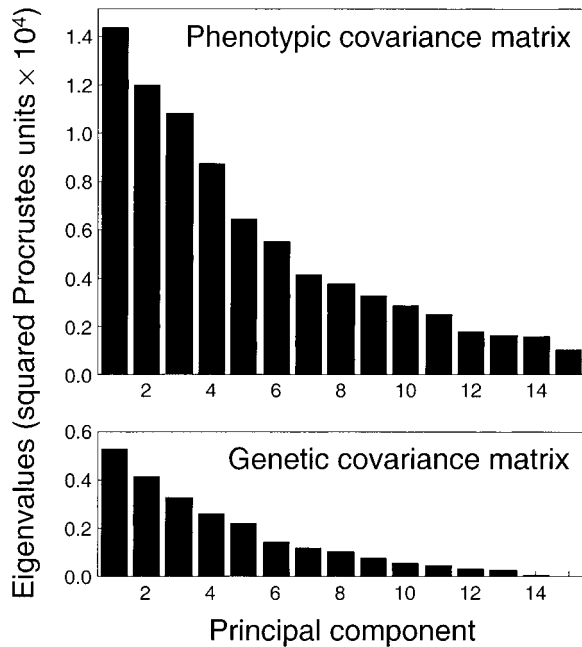


FIG. 3. Eigenvalues of the phenotypic and additive genetic covariance matrices of mandible shape. Note that these are only the first 15 eigenvalues; three more shape dimensions had to be omitted from the analysis, but together make up only 2.4% of the total shape variation.

horizontal in the diagrams presenting the results) and the dorsal-ventral direction perpendicular to it.

## RESULTS

### *Phenotypic and Genetic Variation of Size*

The average centroid size was 15.42 mm, with a standard deviation of 0.74 mm. The additive genetic variance was 0.041 mm<sup>2</sup>, the variance for maternal or litter effects was 0.017 mm<sup>2</sup>, and the residual variance was 0.041 mm<sup>2</sup>. Accordingly, the heritability of centroid size was 0.42 and its standard error was 0.04.

### *Phenotypic and Genetic Variation of Shape*

The amount of phenotypic and genetic variation of shape can best be assessed by examining the eigenvalues of the phenotypic and additive genetic covariance matrices, that is, the amounts of variation associated with the different dimensions in shape space (Fig. 3). For both matrices, much of the variation was concentrated in the first few PCs, but the genetic covariance matrix showed the stronger tendency for the last few eigenvalues to taper off toward zero. The total variance of the phenotypic covariance matrix was  $8.05 \times 10^{-4}$ , that of the additive genetic covariance matrix was  $2.35 \times 10^{-4}$ , and that of the maternal covariance matrix was  $0.64 \times 10^{-4}$  (in dimensionless units of squared Procrustes distance). These total amounts indicate that the additive genetic component accounted for slightly less than a third of the total phenotypic variation; however, we emphasize that the ratio of these sums of variances over the dimensions of shape space cannot be interpreted as an estimate of the her-

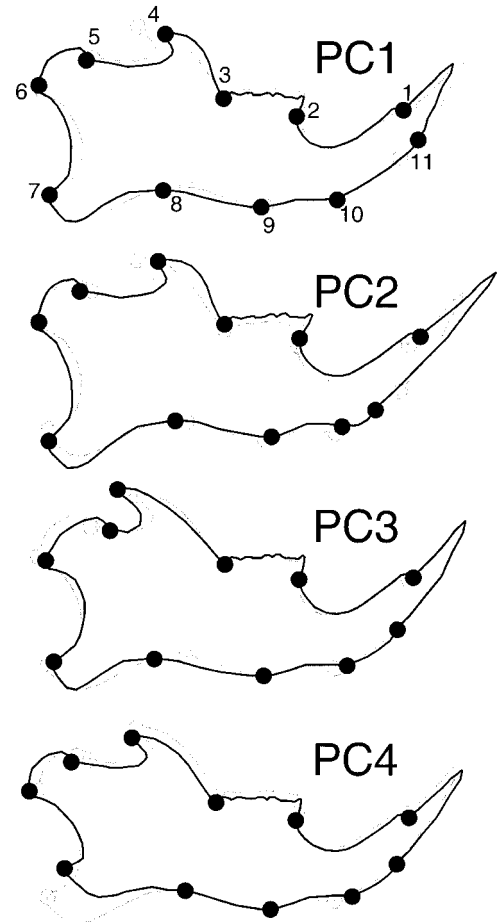


FIG. 4. Principal components (PCs; i.e., eigenvectors) of the phenotypic covariance matrix. The PCs are shown as shape change from the overall average shape in the dataset (open circles, gray outline) to a hypothetical shape with a score of +0.1 for the corresponding PC (solid circles, black outline). This deformation of 0.1 Procrustes units is a very large shape change relative to the variation in the sample. Note that the sign of the PCs is arbitrary: The shifts at every landmark could just as well be graphed all in the opposite directions, but only the shape change in one direction is presented here to save space.

itability of shape (the concept of heritability has no direct equivalent in the multivariate context, and the heritabilities of scalar shape variables can differ widely from this value; see below).

The additive genetic covariance matrix was generally similar to the phenotypic covariance matrix, as indicated by their matrix correlation of 0.88 ( $P < 0.0001$ ). To some extent, this high matrix correlation was due to the part-whole relationship between the two matrices, but there were also fairly high matrix correlations between the additive genetic and maternal covariance matrix ( $MC = 0.74$ ,  $P < 0.0001$ ), as well as between the additive genetic and residual covariance matrices ( $MC = 0.74$ ,  $P < 0.0001$ ).

The shape changes associated with the first four PCs of the phenotypic covariance matrix were varied and tended to affect landmarks in different parts of the mandible simultaneously (Fig. 4). For instance, the PC1 included joint shifts of landmark 4 in the coronoid process, landmark 8 at the

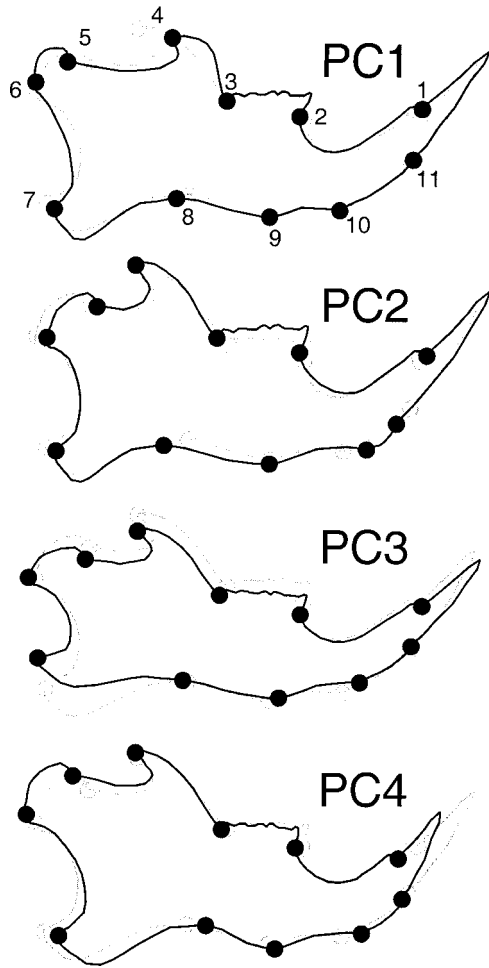


FIG. 5. Principal components (PCs; i.e., eigenvectors) of the additive genetic covariance matrix. Each of the diagrams shows the change from the average shape (open circles, gray outline) to the configuration with a score of +0.1 for the respective PC (solid circles, black outline). For further details, see the the legend of Figure 4.

ventral side of the mandible, and landmark 11 at the insertion of the incisor. Except for landmark 11, the greatest landmark shifts for these four PCs were mostly concentrated in the ascending ramus. Whereas many of these changes appeared to affect landmarks that are in no obvious spatial relation to each other, others clearly seemed to be patterned, for instance, the dorso-ventral compression of the ascending ramus and molar region in the PC 4.

The patterns of variation that were found in the PCs of the additive genetic covariance matrix (Fig. 5) were fairly similar to those of the phenotypic covariance matrix. The PC1s of the phenotypic and genetic covariance matrices clearly corresponded to each other (vector correlation = 0.72, angle  $\alpha = 44.2^\circ$ ,  $P = 0.0019$ ), the PC3 of the phenotypic covariance matrix matched the PC2 of the genetic covariance matrix ( $VC = 0.71$ ,  $\alpha = 45.0^\circ$ ,  $P = 0.0026$ ), and the PC4 of the phenotypic covariance matrix was similar to the PC3 of the genetic covariance matrix ( $VC = 0.74$ ,  $\alpha = 42.4^\circ$ ,  $P = 0.0012$ ). There was no unambiguous match, however, for the PC2 of the phenotypic covariance matrix and the PC4 of the genetic

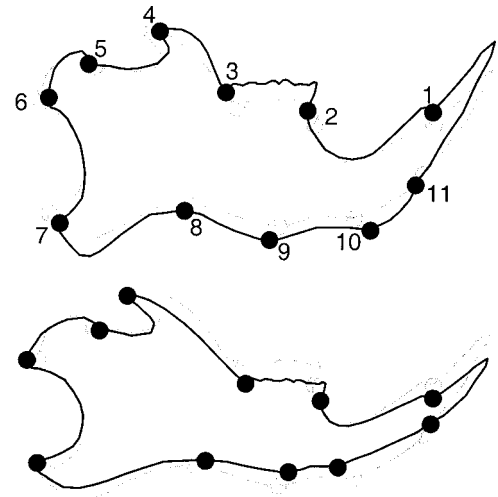


FIG. 6. The shape feature that has the maximal response to selection. When used as a selection differential, this shape variable (calculated as the dominant eigenvector of the matrix  $\mathbf{GP}^-$ ) yields a greater response than any other selection differential of the same magnitude (see text for details), and the response is in the same direction. The diagrams show configurations along this shape vector (solid circles, black outline) at values of +0.1 and -0.1 Procrustes units from the average shape in the dataset (open circles, gray outline).

covariance matrix. Together with the overall comparisons of the covariance matrices, these results suggest that the genetic and phenotypic patterns of variation are similar, but not identical.

*Predicted Response to Selection*

The breeders' equation can be used as another tool to explore the genetic and phenotypic covariance matrices in terms of their potential to respond to selection in the short term. First, we identified the shape feature that would respond most easily to selection (Fig. 6). It is primarily a dorso-ventral expansion or compression of the mandible, combined with weaker anterior-posterior shifts especially of the coronoid and angular processes. Because this shape feature was computed as the dominant eigenvector of the matrix  $\mathbf{GP}^-$ , the selection response would be simply proportional if it were used as the selection differential (i.e., there would be no correlated response according to the partition shown in Fig. 2). The associated eigenvalue of  $\mathbf{GP}^-$  was 0.73 and corresponds to the ratio between the selection differential and the elicited response, that is, the heritability of this particular shape variable. The remaining eigenvalues of this matrix formed a series gradually decreasing toward zero (Fig. 7), but most of them had values indicating that selection in most directions of the shape space would yield an appreciable direct response. The last eigenvalue is of negligible magnitude, but we urge caution in interpreting the last few eigenvalues, because the dimensions of minimal variation may have been affected substantially by error in measurement and variance component estimation and because three additional dimensions were ignored in this analysis.

We computed the predicted responses in six examples of hypothetical selection differentials (Fig. 8). In the first two

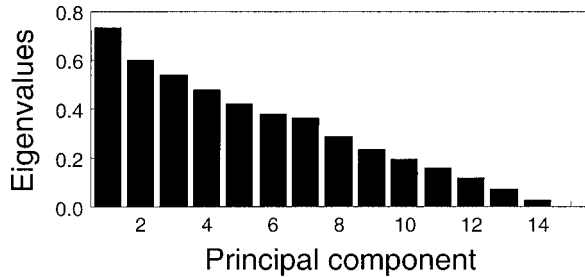


FIG. 7. Eigenvalues of the matrix  $GP^-$ . These can be interpreted as the heritabilities of the shape variables corresponding to the principal components of the matrix  $GP^-$ . Because most of the eigenvalues are clearly greater than zero, most shape dimensions are accessible to selection, that is, there will be a direct response to selection for the corresponding shape features.

scenarios, the selection differentials consisted exclusively of shifts in the position of a single landmark on the condylar process (landmark 6) in either posterior (Fig. 8A) or dorsal direction (Fig. 8B). The magnitude of predicted responses for both these selection differentials corresponded to about 30% and 40% of the selection differential, respectively, but in both cases the correlated response exceeded the direct response. Landmark 6 moved in the direction selected in both cases, but the correlated shifts of other landmarks were markedly different between the two examples. In case A, the greatest correlated shifts were at landmarks 2 and 8, and smaller shifts occurred in landmarks 1, 3, and 11 and thus extended through all major parts of the mandible. In contrast, the correlated response for case B was primarily confined to the region affected by selection, namely to landmarks 4 and 5 in the coronoid and condylar processes.

The third scenario featured a selection differential with a joint dorsal and posterior movement of landmarks 1 and 11 at the insertion of the incisor, leading to a more pronounced bending of the anterior part of the mandible including the incisor alveolus (Fig. 8C). The predicted response was somewhat smaller than in the preceding examples, and the correlated response also exceeded the direct response. The correlated response involved slight downward shifts of landmarks 8–10 along the lower contour of the mandible, thus attenuating the bending near landmark 10, as well as displacements of landmark 2 at the insertion of the first molar and landmark 4 in the coronoid process.

Whereas the selection differentials in the previous examples were designed arbitrarily to examine the role of the geometric of selection, the following examples were intended to reproduce two patterns of variation found to recur in the analyses of this study (Figs. 4 and 5), in the effects of multiple QTLs on mandible shape, and in the phenotypes produced by several gene knockout experiments (discussed in Klingenberg et al. 2001b). One of these recurrent patterns was a shift of landmark 4 mostly in anterior direction that corresponds to a reduction of the coronoid process (Fig. 8D) relative to the angular and condylar processes (similar shifts exist for the angular process, but here we did not simulate that pattern). The second pattern is a dorso-ventral compression (or a simultaneous reduction) of the angular and coronoid processes (landmarks 4 and 7; Fig. 8E). In both cases, the components of direct response to selection ex-

ceeded those of the correlated response, because the landmarks affected by the selection differential were the only ones that showed a substantial response.

The last selection differential was set up according to the muscle hypertrophy model for differences in mandible shape between mice and rats (Atchley et al. 1992, p. 211). In this model, the area of muscle attachment in the ascending ramus expands relative to other components of the mandible, which was reflected in the selection differential by a dorsal and posterior shift of landmark 4 at the coronoid process, a ventral and posterior shift of landmark 7 at the angular process, and a simultaneous anterior movement of landmarks 3 and 8 (Fig. 8F). As in the preceding two examples, the direct component of the predicted response for this selection differential exceeded the component of the correlated response. The correlated response was distributed throughout the mandible and included changes both in the alveolar process (especially landmarks 1 and 10) and at the condylar process (landmark 5).

## DISCUSSION

This study applied the methods of geometric morphometrics in the context of quantitative genetics of the mouse mandible. For the analysis of overall size, standard quantitative genetic methods can be applied, and our heritability estimate of 0.42 is comparable to the estimates obtained by Leamy (1974) for mandible length in the same set of mice. For analyses of shape, it is possible to combine the methods of geometric morphometrics with the multivariate theory of quantitative genetics (Lande 1979; Lande and Arnold 1983; Cheverud 1984) because the data from Procrustes superimposition are amenable to the analyses of classical multivariate statistics (e.g., Bookstein 1996; Dryden and Mardia 1998). Moreover, the development of effective methods for estimating genetic covariance matrices even from unbalanced or nonstandard breeding designs has made this kind of study feasible (e.g., Shaw 1987; Lynch and Walsh 1998; Neumaier and Groeneveld 1998). We emphasize, however, that the high dimensionality of morphometric analyses with more than just a few landmarks renders any such investigation an ambitious undertaking. Studies of this sort are therefore extremely data hungry and require large breeding designs, preferably with hundreds of sufficiently large families.

The overall comparison by matrix correlation indicates that the phenotypic and genetic covariance matrices are fairly similar to each other. The comparison of the first four PCs further underscores this similarity, but also shows that they are not identical. This is consistent with the findings of earlier studies in the mouse mandible (Bailey 1956) and various skeletal traits (Leamy 1977; the same mice as were used in this study), in mouse and rat pelvic measurements (Kohn and Atchley 1988), as well as a range of measurements in other animals (Cheverud 1988; Roff 1997, p. 95 ff.). Such similarity has been interpreted as evidence that both genetic and environmental variation are expressed phenotypically through the same processes. In agreement with this view, correspondence of patterns of variation has also been reported between the individual variation and fluctuating asymmetry in these mice (Leamy 1993) and in other animals (Klingen-

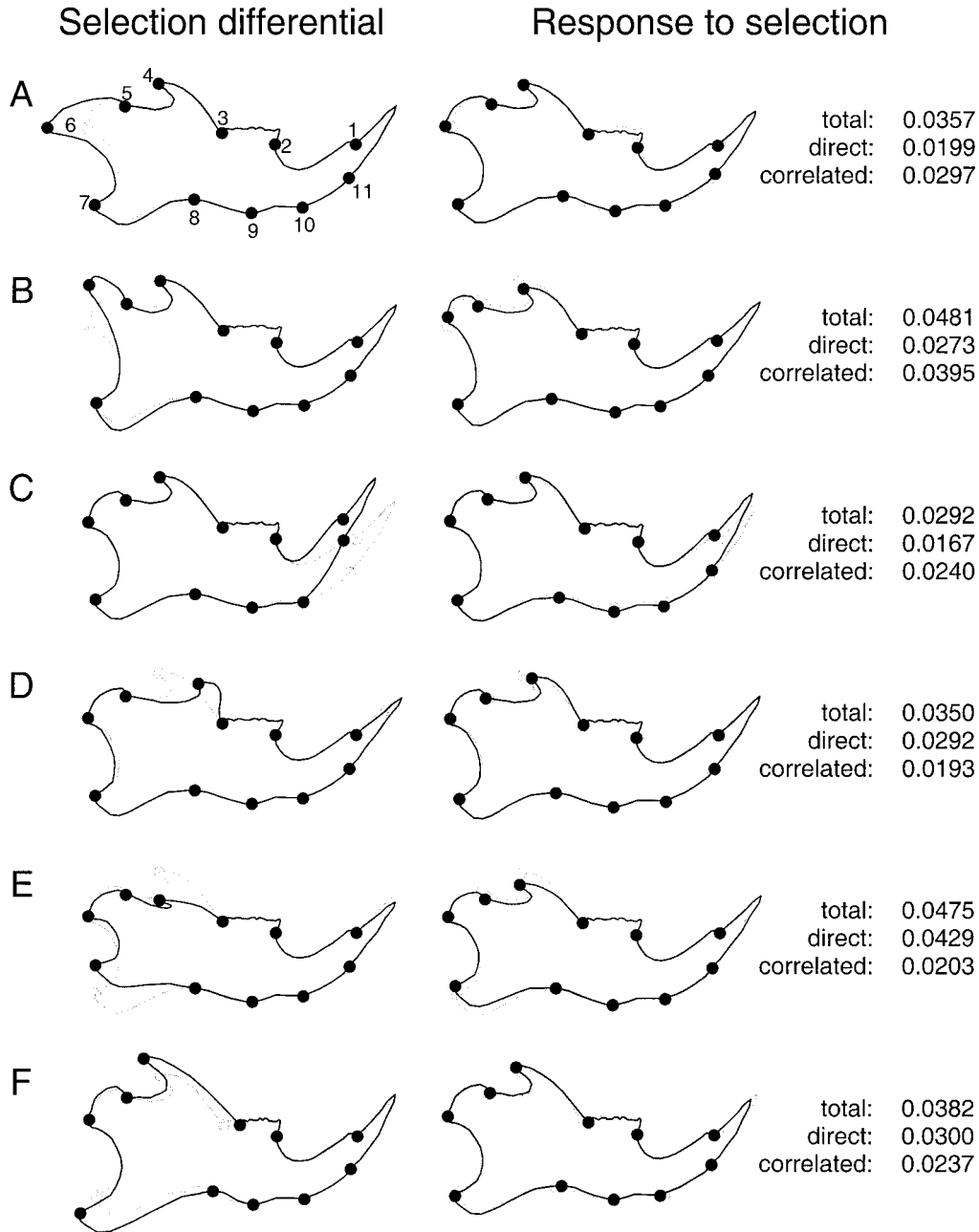


FIG. 8. Predicted responses to selection on six different shape features. For each case, the diagram on the left shows the selection differential, and the diagram on the right presents the response to selection (open circles and gray outlines: average shape before selection; solid circles and black outlines: average shape of selected parents or of the offspring generation). Each selection differential is a shape change that corresponds to a Procrustes distance of 0.12. The values to the right indicate the magnitude of the total response to selection and its components of direct and correlated responses in units of Procrustes distance (for details, see text and Fig. 2).

berg and McIntyre 1998; Klingenberg and Zaklan 2000; Klingenberg et al. 2001a), suggesting that genetic and environmental differences among individuals as well as random variation within them may affect the same developmental pathways (but see also Debat et al. 2000).

This line of argument is further strengthened by the observation that the PCs of the genetic and phenotypic covariance matrices include two recurrent patterns previously identified from the effects of multiple loci in a QTL study of

mandible shape in mice and from the phenotypes resulting from gene knockout experiments (Klingenberg et al. 2001b). The first of these patterns is a dorso-ventral compression or expansion at the coronoid and angular processes (Fig. 4, PC4; Fig. 5, PC3). This effect also appeared in multiple QTLs (Klingenberg et al. 2001b) and in the knockout effects for genes such as *gooseoid* (Rivera-Pérez et al. 1999) or *Gli2* and *Gli3* (Mo et al. 1997), among others. The second pattern is an opposite anterior-posterior movement of the coronoid

and angular processes or an independent anterior-posterior movement of only one of these landmarks (Fig. 4, PC1, PC2, PC3; Fig. 5, PC1, PC4). It also is manifest in the effects of several QTLs for mandible shape (Klingenberg et al. 2001b) and in the knockout phenotypes for genes such as *Dlx5* (Acampora et al. 1999; Depew et al. 1999) or *TGF $\beta$ 2* (Sanford et al. 1997). Because of the different experimental contexts in which these same patterns have been found, it appears that they are the expression of variation in pathways that play a role in the development of the mandible, and that various changes in each of those pathways can produce similar results. In this view, the developmental system would channel variation of diverse origins to be expressed in these recurrent phenotypic patterns (e.g., Riska 1986; Klingenberg, in press).

Neither the additive genetic nor the phenotypic covariance matrices alone are sufficient to predict the response to selection according to the multivariate breeders' equation  $\Delta\boldsymbol{\mu} = \mathbf{G}\mathbf{P}^{-1}\mathbf{s}$ , because the crucial factor is the relationship between them. For instance, if the two matrices are proportional so that  $\mathbf{G} = c\mathbf{P}$  (where  $0 < c < 1$ ), then  $\mathbf{G}\mathbf{P}^{-1} = c\mathbf{I}$  (where  $\mathbf{I}$  is an identity matrix), and it follows that  $\Delta\boldsymbol{\mu} = c\mathbf{s}$ , implying that any selection differential will elicit a directly proportional response. What determines how the selection differential translates into a selection response is the additive genetic variation scaled in relation to the phenotypic variation in the population (e.g., Cheverud 1984; Cowley and Atchley 1990). In our study, this is clearly reflected by the observation that the shape feature that would most easily respond to selection (Fig. 6) does not coincide with any one of the major axes of the genetic or phenotypic covariance matrices (Figs. 4, 5), although some shape changes in parts of the mandible are similar. Moreover, the eigenvalues of the matrix  $\mathbf{G}\mathbf{P}^{-1}$  (Fig. 7) form a more linear graduated series than those of either the  $\mathbf{P}$  or  $\mathbf{G}$  matrices (Fig. 3), for which variation is more concentrated in the first few dimensions. Apparently, this greater genetic and phenotypic variation in some dimensions of shape space partly cancels out when the two matrices are combined.

The eigenvalues of the matrix  $\mathbf{G}\mathbf{P}^{-1}$  can be interpreted as the heritabilities of the shape variables corresponding to the respective PCs (eigenvectors). These eigenvalues (Fig. 7) cover just about the entire range of heritabilities reported for morphological traits in animals (e.g., Mousseau and Roff 1987; Roff 1997, ch. 2). They are a reminder that there is not a single measure of heritability for shape per se, but that there is a range of values for heritability depending on the particular shape variable of interest. Heritability, as a univariate measure, is only of limited utility in the multivariate context of shape analysis.

The responses to selection on various shape features illustrate the need for caution against uncritically adopting univariate approaches in shape studies and reveal several important lessons for the quantitative genetics of shape (Fig. 8). These examples particularly highlight the importance of how shape change by selection relates to the geometry of the mandible. The first two examples make this especially clear (Figs. 8A, B): The selection differentials are both shifts of landmark 6 at the condylar process and of the same magnitude, but they are at right angles to each other. If selection is for a shift to a more dorsal position, then the shape change

due to the correlated response is primarily confined to the neighboring landmarks 4 and 5 in the condylar and angular processes (Fig. 8B). In contrast, if the selection differential is a dorsal movement of the same landmark, the response is a general dorso-ventral narrowing that extends far into the anterior portion of the mandible (Fig. 8A). Applying selection differentials at the same landmark but in different directions therefore can yield responses that are fundamentally different shape changes.

The selection response is not necessarily restricted to the neighborhood of the landmarks affected by the selection differential. In the example of Fig. 8A, selection affecting a landmark in the posterior part of the mandible generates a response that extends along the entire length of the mandible, and in the example of Figure 8C, selection for a dorsal shift of the anteriormost two landmarks yields a change in landmark 4 at the coronoid process (the remaining examples in Fig. 8 also show subtle effects of this sort). These examples also show that the correlated response to selection can extend over considerable distances and can even transgress the anatomical and functional subdivision of the mandible into the alveolar process and the ascending ramus (Fig. 1). This result contrasts with evidence for a considerable degree of genetic autonomy of each of these parts, for instance, the finding that a majority of QTLs affecting the interlandmark distances in the mandible has effects that are confined either to the ascending ramus or to the alveolar process (Cheverud et al. 1997; Mezey et al. 2000). Our result is thus closer to the findings of a QTL study using the same geometric approach, which did not reveal clustering of QTLs into separate groups affecting the two parts of the mandible (Klingenberg et al. 2001b).

The correlated response, as defined in Figure 2, constitutes a substantial proportion of the total response to selection in all these examples (Fig. 8). This means that the total response is usually a shape change considerably different from the selection differential, either because different landmarks are involved or because landmarks move in different directions. In some cases, it is possible to suggest possible causes for these correlated responses. For example, in Figure 8C, it is conceivable that the ventral shifts of landmarks 8 and 9 occur because sharp bending of the mandible at an angle near landmark 10 is structurally impossible due to the constant curvature of the incisor alveolus, which extends back as an arc inside the body of the mandible (cf. Fig. 1). Similarly, variation in the degree to which the maxillary incisor protrudes forward from the skull in rodents is due to joint changes in the the curvature of the tooth and in the position of the incisor root (Landry 1957; Lessa and Patton 1989).

In the first three examples, which were designed exclusively according to geometric criteria, the correlated responses are particularly extensive and consistently exceed the direct response in magnitude (Figs. 8A–C). In contrast, for each of the other three examples (Figs. 8D–F), the direct response is greater than the correlated response. Those examples were intended to reflect recurring shape features of QTL effects (Figs. 8D, E; Klingenberg et al. 2001b) and a pattern of functional variation (muscle hypertrophy) and differentiation between mice and rats (Fig. 8F; Atchley et al. 1992, p. 211). Therefore, these shape features represent the patterns of po-

tentially available genetic variation or of a realized evolutionary change, respectively. That these patterns are more effective at producing a direct response than selection differentials designed as arbitrary geometric changes may be viewed as a manifestation of genetic constraints reflecting the development and anatomical structure of the mandible.

These hypothetical examples show that the correlated response not only is a substantial part of the total effect of selection, but it also carries critical information on the geometry of the selection response, making it possible to consider the evolutionary potential in terms of the anatomical structure of the mandible. This important aspect of shape is entirely ignored by studies selecting one or more shape measures at the outset and then using univariate methods for each separately, either with the techniques of classical quantitative genetics (e.g., Arnqvist and Thornhill 1998; Currie et al. 2000) or with QTL approaches (e.g., Liu et al. 1996; Laurie et al. 1997; Weber et al. 1999; Birdsall et al. 2000; Zeng et al. 2000; Zimmerman et al. 2000). Unless there is a compelling reason why only one shape feature is of interest in a study, such as the difference in the shape averages between two species (Liu et al. 1996; Laurie et al. 1997; Zeng et al. 2000), we strongly recommend the multivariate approach to the analysis of shape. In this paper, we have demonstrated the methods to study multidimensional shape in the context of classical quantitative genetics, and the corresponding approach in the context of QTL analyses is described elsewhere (Klingenberg et al. 2001b). We are confident that this perspective will yield novel insights into the genetic basis of adaptive change in morphological structures and its developmental underpinning.

#### ACKNOWLEDGMENTS

We thank J. Purtell for patiently digitizing the mandibles and N. Goldman for access to computer resources. We are grateful to J. K. K. Merilä and two anonymous reviewers for constructive comments that helped us to improve the paper. Financial support was provided by a grant from the Long Beach California State University Foundation to L.J.L. and by a fellowship from the Human Frontier Science Program to CPK.

#### LITERATURE CITED

- Acampora, D., G. R. Merlo, L. Paleari, B. Zerega, M. P. Postiglione, S. Mantero, E. Bober, O. Barbieri, A. Simeone, and G. Levi. 1999. Craniofacial, vestibular and bone defects in mice lacking the *Distal-less* related gene *Dlx5*. *Development* 126:3795–3809.
- Arnqvist, G., and R. Thornhill. 1998. Evolution of animal genitalia: patterns of phenotypic and genotypic variation and condition dependence of genital and non-genital morphology in water strider (Heteroptera: Gerridae: Insecta). *Genet. Res.* 71:193–212.
- Atchley, W. R., and B. K. Hall. 1991. A model for development and evolution of complex morphological structures. *Biol. Rev.* 66:101–157.
- Atchley, W. R., A. A. Plummer, and B. Riska. 1985. Genetics of mandible form in the mouse. *Genetics* 111:555–577.
- Atchley, W. R., D. E. Cowley, E. J. Eisen, H. Prasetyo, and D. Hawkins-Brown. 1990. Correlated response in the developmental choreographies of the mouse mandible to selection for body composition. *Evolution* 44:669–688.
- Atchley, W. R., D. E. Cowley, C. Vogl, and T. McLellan. 1992. Evolutionary divergence, shape change, and genetic correlation structure in the rodent mandible. *Syst. Biol.* 41:196–221.
- Bailey, D. W. 1956. A comparison of genetic and environmental principal components of morphogenesis in mice. *Growth* 20:63–74.
- . 1985. Genes that affect the shape of the murine mandible: congenic strain analysis. *J. Hered.* 76:107–114.
- . 1986. Genes that affect morphogenesis of the murine mandible: recombinant-inbred strain analysis. *J. Hered.* 77:17–25.
- Birdsall, K., E. Zimmerman, K. Teeter, and G. Gibson. 2000. Genetic variation for the positioning of wing veins in *Drosophila melanogaster*. *Evol. Dev.* 2:16–24.
- Bookstein, F. L. 1991. Morphometric tools for landmark data: geometry and biology. Cambridge Univ. Press, Cambridge, U.K.
- . 1996. Biometrics, biomathematics and the morphometric synthesis. *Bull. Math. Biol.* 58:313–365.
- Cheverud, J. M. 1984. Quantitative genetics and developmental constraints on evolution by selection. *J. Theor. Biol.* 110:155–171.
- . 1988. A comparison of genetic and phenotypic correlations. *Evolution* 42:958–968.
- . 1996. Developmental integration and the evolution of pleiotropy. *Am. Zool.* 36:44–50.
- . 2001. The genetic architecture of pleiotropic relations and differential epistasis. Pp. 411–433 in G. P. Wagner, ed. *The character concept in evolutionary biology*. Academic Press, San Diego, CA.
- Cheverud, J. M., S. E. Hartman, J. T. Richtsmeier, and W. R. Atchley. 1991. A quantitative genetic analysis of localized morphology in mandibles of inbred mice using finite element scaling. *J. Craniofac. Genet. Dev. Biol.* 11:122–137.
- Cheverud, J. M., E. J. Routman, and D. J. Irschick. 1997. Pleiotropic effects of individual gene loci on mandibular morphology. *Evolution* 51:2006–2016.
- Cowley, D. E., and W. R. Atchley. 1990. Development and quantitative genetics of correlation structure among body parts of *Drosophila melanogaster*. *Am. Nat.* 135:242–268.
- Currie, A. J., S. Ganeshanandam, D. A. Noiton, D. Garrick, C. J. A. Shelbourne, and N. Oraguzie. 2000. Quantitative evaluation of apple (*Malus × domestica* Borkh.) fruit shape by principal component analysis of Fourier descriptors. *Euphytica* 111:219–227.
- Debat, V., P. Alibert, P. David, E. Paradis, and J.-C. Auffray. 2000. Independence between developmental stability and canalization in the skull of the house mouse. *Proc. R. Soc. Lond. B Biol. Sci.* 267:423–430.
- Depew, M. J., J. K. Liu, J. E. Long, R. Presley, J. J. Meneses, R. A. Pedersen, and J. L. R. Rubenstein. 1999. *Dlx5* regulates regional development of the branchial arches and sensory capsules. *Development* 126:3831–3846.
- Dryden, I. L., and K. V. Mardia. 1998. *Statistical analysis of shape*. Wiley, Chichester, U.K.
- Duarte, L. C., L. R. Monteiro, F. J. Von Zuben, and S. F. Dos Reis. 2000. Variation in mandible shape in *Trichomys apereoides* (Mammalia: Rodentia): geometric analysis of a complex morphological structure. *Syst. Biol.* 49:563–578.
- Falconer, D. S., and T. F. C. Mackay. 1996. *Introduction to quantitative genetics*. Longman, Essex, U.K.
- Flury, B. 1997. *A first course in multivariate statistics*. Springer, New York.
- Hall, B. K. 1999. *Evolutionary developmental biology*. Kluwer, Dordrecht, The Netherlands.
- Klingenberg, C. P. 1996. Multivariate allometry. Pp. 23–49 in L. F. Marcus, M. Corti, A. Loy, G. J. P. Naylor, and D. E. Slice, eds. *Advances in morphometrics*. Plenum Press, New York.
- . In press. Developmental instability as a research tool: using patterns of fluctuating asymmetry to infer the developmental origins of morphological integration. In M. Polak, ed. *Developmental instability: causes and consequences*. Oxford Univ. Press, New York.
- Klingenberg, C. P., and G. S. McIntyre. 1998. Geometric morphometrics of developmental instability: analyzing patterns of fluctuating asymmetry.

- tuating asymmetry with Procrustes methods. *Evolution* 52: 1363–1375.
- Klingenberg, C. P., and S. D. Zaklan. 2000. Morphological integration between developmental compartments in the *Drosophila* wing. *Evolution* 54:1273–1285.
- Klingenberg, C. P., A. V. Badyaev, S. M. Sowry, and N. J. Beckwith. 2001a. Inferring developmental modularity from morphological integration: analysis of individual variation and asymmetry in bumblebee wings. *Am. Nat.* 157:11–23.
- Klingenberg, C. P., L. J. Leamy, E. J. Routman, and J. M. Cheverud. 2001b. Genetic architecture of mandible shape in mice: effects of quantitative trait loci analyzed by geometric morphometrics. *Genetics* 157:785–802.
- Kohn, L. A. P., and W. R. Atchley. 1988. How similar are genetic correlation structures? Data from mice and rats. *Evolution* 42: 467–481.
- Lande, R. 1979. Quantitative genetic analysis of multivariate evolution, applied to brain: body size allometry. *Evolution* 33: 402–416.
- Lande, R., and S. J. Arnold. 1983. The measurement of selection on correlated characters. *Evolution* 37:1210–1226.
- Landry, S. O., Jr. 1957. Factors affecting the procumbency of rodent upper incisors. *J. Mammal.* 38:223–234.
- Laurie, C. C., J. R. True, J. Liu, and J. M. Mercer. 1997. An introgression analysis of quantitative trait loci that contribute to a morphological difference between *Drosophila simulans* and *D. mauritiana*. *Genetics* 145:339–348.
- Leamy, L. 1974. Heritability of osteometric traits in a randombred population of mice. *J. Hered.* 65:109–120.
- . 1977. Genetic and environmental correlations of morphometric traits in random-bred house mice. *Evolution* 31:357–369.
- . 1993. Morphological integration of fluctuating asymmetry in the mouse mandible. *Genetica* 89:139–153.
- . 1999. Heritability of directional and fluctuating asymmetry for mandibular characters in random-bred mice. *J. Evol. Biol.* 12:146–155.
- Leamy, L., and D. Bradley. 1982. Static and growth allometry of morphometric traits in random-bred house mice. *Evolution* 36: 1200–1212.
- Lessa, E. P., and J. L. Patton. 1989. Structural constraints, recurrent shapes, and allometry in pocket gophers (genus *Thomomys*). *Biol. J. Linn. Soc.* 36:349–363.
- Liu, J., J. M. Mercer, L. F. Stam, G. C. Gibson, Z.-B. Zeng, and C. C. Laurie. 1996. Genetic analysis of a morphological shape difference in the male genitalia of *Drosophila simulans* and *D. mauritiana*. *Genetics* 142:1129–1145.
- Lynch, M., and B. Walsh. 1998. *Genetics and analysis of quantitative traits*. Sinauer, Sunderland, MA.
- Mezey, J. G., J. M. Cheverud, and G. P. Wagner. 2000. Is the genotype-phenotype map modular? A statistical approach using mouse quantitative trait loci data. *Genetics* 156:305–311.
- Milner, J. M., J. M. Pemberton, J. M. Brotherstone, and S. D. Albon. 2000. Estimating variance components and heritabilities in the wild: a case study using the ‘animal model’ approach. *J. Evol. Biol.* 13:804–813.
- Mitchell-Olds, T., and R. G. Shaw. 1987. Regression analysis of natural selection: statistical inference and biological interpretation. *Evolution* 41:1149–1161.
- Mo, R., A. M. Freer, D. L. Zinyk, M. A. Crackower, J. Michaud, H. H.-Q. Heng, K. W. Chik, X.-M. Shi, L.-C. Tsui, S. H. Cheng, A. L. Joyner, and C.-C. Hui. 1997. Specific and redundant functions of *Gli2* and *Gli3* zinc finger genes in skeletal patterning and development. *Development* 124:113–123.
- Mousseau, T. A., and D. A. Roff. 1987. Natural selection and the heritability of fitness components. *Heredity* 59:181–197.
- Neumaier, A., and E. Groeneveld. 1998. Restricted maximum likelihood estimation of covariances in sparse linear models. *Genet. Sel. Evol.* 30:3–26.
- Riska, B. 1986. Some models for development, growth, and morphometric correlation. *Evolution* 40:1303–1311.
- Rivera-Pérez, J. A., M. Wakamiya, and R. R. Behringer. 1999. *Gooseoid* acts cell autonomously in mesenchyme-derived tissues during craniofacial development. *Development* 126: 3811–3821.
- Roff, D. A. 1997. *Evolutionary quantitative genetics*. Chapman and Hall, New York.
- Sanford, L. P., I. Ormsby, A. C. Gittenberger-de Groot, H. Sariola, R. Friedman, G. P. Boivin, E. L. Cardell, and T. Doetschman. 1997. TGF $_2$  knockout mice have multiple developmental defects that are non-overlapping with other TGF $_$  knockout phenotypes. *Development* 124:2659–2670.
- Shaw, R. G. 1987. Maximum-likelihood approaches applied to quantitative genetics of natural populations. *Evolution* 41: 812–826.
- Weber, K., R. Eisman, L. Morey, A. Patty, J. Sparks, M. Tausek, and Z.-B. Zeng. 1999. An analysis of polygenes affecting wing shape on chromosome 3 in *Drosophila melanogaster*. *Genetics* 153:773–786.
- Zeng, Z.-B., J. Liu, L. F. Stam, C.-H. Kao, J. M. Mercer, and C. C. Laurie. 2000. Genetic architecture of a morphological shape difference between two *Drosophila* species. *Genetics* 154: 299–310.
- Zimmerman, E., A. Palsson, and G. Gibson. 2000. Quantitative trait loci affecting components of wing shape in *Drosophila melanogaster*. *Genetics* 155:671–683.

Corresponding Editor: J. Merilä